Peroxynitrite Reductase Activity of Selenoprotein Glutathione Peroxidase: A Computational Study†

Rajeev Prabhakar, Keiji Morokuma, and Djamaladdin G. Musaev*

Cherry L. Emerson Center for Scientific Computation and Department of Chemistry, Emory University, 1515 Dickey Drive, Atlanta, Georgia 30322

Received March 7, 2006; Revised Manuscript Received April 12, 2006

ABSTRACT: The peroxynitrite reductase activity of selenoprotein glutathione peroxidase (GPx) has been investigated using density functional theory calculations for peroxynitrite/peroxynitrous acid ($ONOO^-$/ONOOH) substrates through two different "oxidation" and "nitration" pathways. In the oxidation pathway for $ONOO^-$, the oxidation of GPx and the subsequent formation of the selenenic acid (E−Se−OH) occur through a concerted mechanism with an energy barrier of 4.7 (3.7) kcal/mol, which is in good agreement with the computed value of 7.1 kcal/mol for the drug ebselen and the experimentally measured barrier of 8.8 kcal/mol for both ebselen and GPx. For ONOOH, the formation of the E−Se−OH prefers a stepwise mechanism with an overall barrier of 6.9 (11.3) kcal/mol, which is 10.2 (11.2) kcal/mol lower than that for hydrogen peroxide (H_2O_2), indicating that ONOOH is a more efficient substrate for GPx oxidation. It has been demonstrated that the active site Gln83 residue plays a critical role during the oxidation process, which is consistent with the experimental suggestions. The nitration of GPx by ONOOH produces a nitro (E−Se−NO_2) product via either of two different mechanisms, isomerization and direct, having almost the same barrier heights. A comparison between the rate-determining barriers of the oxidation and nitration pathways suggests that the oxidation of GPx by ONOOH is more preferable than its nitration. It was also shown that the rate-determining barriers remain the same, 21.5 (25.5) kcal/mol, in the peroxynitrite reductase and peroxidase activities of GPx.

Glutathione peroxidase (GPx)[1] is a selenoprotein, which demonstrates a strong antioxidant activity and protects cell membranes and other cellular components against oxidative damage (*2*, *3*). It reduces numerous reactive oxygen species (ROS) including hydrogen peroxide (*1*) and peroxynitrite (*4*) by utilizing various reducing substrates. The peroxidase activity of GPx has been studied extensively (*5*). However, the elucidation of its peroxynitrite reductase activity still requires more comprehensive experimental and theoretical investigations. Therefore, in the present study, the mechanism and factors controlling the peroxynitrite reductase activity of GPx have been theoretically investigated.

Peroxynitrite anion[2] ($ONOO^-$), formed by the direct and rapid combination of nitric oxide (NO) and superoxide anion (O_2^-), is a potent cytotoxic agent which has attracted a great interest over the past decades (*5*, *6*). It is stable in alkaline solution, but under physiological conditions it quickly protonates and forms peroxynitrous acid (OONOH). OONOH undergoes rapid homolysis, with a rate constant of 1.3 s^{-1} (*3*), to give OH• and NO_2• radical pairs (*6*−*8*). Both $ONOO^-$ and ONOOH, as well as the related radicals (OH•, NO_2•, and CO_3•) formed during the reaction of $ONOO^-$ with a CO_2 molecule (*9*−*11*), react rapidly with numerous biomolecules (*12*−*20*) and are proposed to be involved in many disease states (*5*, *6*). An intensive search for catalysts to detoxify this powerful oxidizing and nitrating agent has demonstrated that selenoproteins (for example, GPx) (*21*) and some heme-containing proteins (*22*), as well as a series of water-soluble Fe(III) porphyrin complexes (*23*), synthetic organo-selenium compounds (*24*) [for example, ebselen [2-phenyl-1,2-benzisoselenazol-3(2*H*)-one]] (*25*−*27*), and organo-sulfur compounds (for example, methionine, glutathione) (*28*) can intercept $OONO^-$ and/or catalyze its decomposition and isomerization. Among all of these catalysts GPx enzyme has been found to be very promising (*29*). Therefore, a better understanding of the peroxynitrite reductase activity of this enzyme is extremely important as it will further advance efforts for the discovery of better drugs.

In general, four different classes of Se-dependent GPx, (1) cytosolic (GPx-1), (2) gastrointestinal tract (GPx-2), (3) extracellular (GPx-3), and (4) phospholipid hydroperoxide (GPx-4), have been classified in the literature (*4*). However, the crystal structures of only bovine erythrocyte (intracellular enzyme, GPx-1) and human plasma (extracellular enzyme, GPx-3) GPx have been resolved (*30*, *31*). These studies show that the enzymes are tetrameric, with two asymmetric units containing two dimers that exhibit half-site reactivity, and each monomer has a critical selenocysteine residue, which is explicitly involved in the catalytic cycle (*32*−*36*). The

† This research was supported by a grant from the National Science Foundation (CHE-0209660).

* To whom correspondence should be addressed: e-mail, dmusaev@emory.edu; tel, 404-727-2382; fax, 404-727-7412.

[1] Abbreviations: GPx, glutathione peroxidase; GSH, glutathione; DFT, density functional theory; TS, transition state; ROS, reactive oxygen species.

[2] The term peroxynitrite is used to refer to the peroxynitrite anion, O═NOO^-, and peroxynitrous acid, ONOOH, unless otherwise indicated. The IUPAC recommended names are oxoperoxonitrate(1−) and hydrogen oxoperoxonitrate, respectively.

10.1021/bi060456e CCC: $33.50
Published on Web 05/13/2006

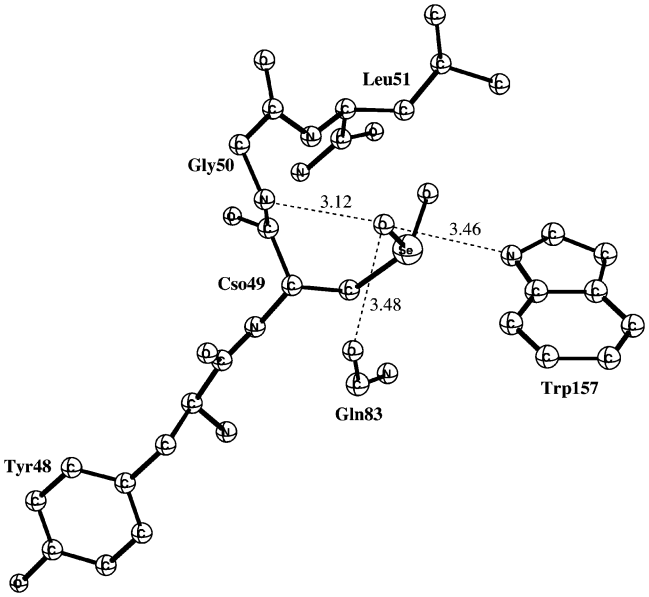

FIGURE 1: X-ray structure of the active site region of GPx.

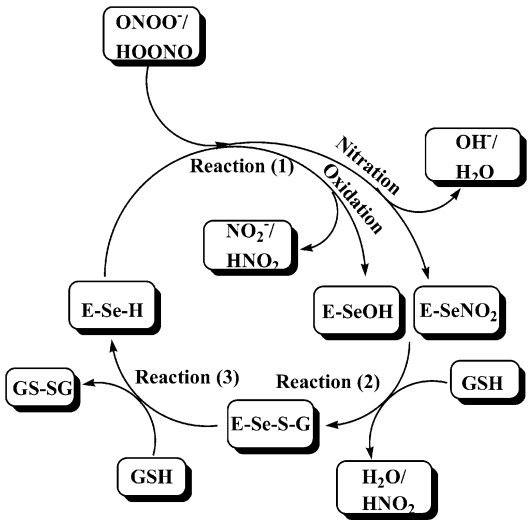

FIGURE 2: Experimentally suggested mechanism for the catalytic cycle of peroxynitrite/peroxynitrous acid reductase by GPx.

X-ray structure of the active site of human plasma GPx is shown in Figure 1. As shown in this figure, the selenocysteine residue of the enzyme exists in the "resting" seleninic acid, E−Se(O)(OH), form. The active site Gln83 and Trp157 residues are located within hydrogen-bonding distance to the selenium atom and have been suggested to play a critical role in the catalysis (*30*). These two residues are known to be conserved in the entire glutathione peroxidase superfamily and their homologues, which probably account for the similarities in their catalytic mechanisms (*37*). The active site seleninic acid residue is coordinated to Gly50 and Tyr48 in a tetradic arrangement (*31*). It has been experimentally suggested that the catalytically active form of GPx is either selenolate anion (E−Se^-) or selenol (E−SeH) (*30*).

On the basis of the extensive experimental (*29*−*31*, *38*) and theoretical (*39*) information for the peroxidase activity of GPx, the proposed catalytic mechanism for peroxynitrite/peroxynitrous acid ($ONOO^-$/ONOOH) reduction by this enzyme is shown in Figure 2. The suggested mechanism incorporates the fact that under physiological conditions peroxynitrite reductase activity of GPx in vivo can follow either the "oxidation" or "nitration" of the critical selenocysteine residue (*30*, *38*). Therefore, throughout the paper these two processes are referred as oxidation and nitration pathways, respectively. As discussed below only the first step, reaction 1, of these pathways is completely different. In the oxidation pathway, $ONOO^-$/ONOOH reduction is accompanied by the oxidation of the selenol (E−SeH) to the selenenic acid (E−Se−OH), whereas in the nitration pathway, the seleocysteine residue is nitrated by $ONOO^-$/ONOOH to generate E−Se−NO_2. For substrate $ONOO^-$, the experimentally measured rate for the formation of E−Se−OH expressed per monomer of reduced GPx of $(2.0 \pm 0.2) \times 10^6$ M^{-1} s^{-1} corresponds to a barrier of 8.8 kcal/mol (*29*). After the oxidation or nitration of the selenocysteine residue, the subsequent chemistry, reactions 2 and 3 (see Figure 2), in both pathways is similar. In the second step, reaction 2, substrate glutathione (GSH) reacts with E−Se−OH or E−Se−NO_2 to produce a seleno−sulfide adduct (E−Se−SG), which has been observed recently (*36*). In the third step, reaction 3, a second molecule of GSH attacks the seleno−sulfide adduct to regenerate the active form of the enzyme and form disulfide GS−SG.

In the present study, we have applied high-level quantum chemical approaches incorporating all of the available experimental information to investigate the reaction mechanisms of the peroxynitrite reductase activity of GPx through oxidation and nitration pathways. The results presented in this study not only allow a detailed analysis of the individual steps of the mechanism but also provide energetics and structures of all short-lived intermediates and transition states. Since this work is the continuation of our previous studies on $ONOO^-$/ONOOH reduction by the antiinflammatory drug ebselen (*40*, *41*) and the catalytic cycle of peroxidase activity of GPx (*39*), in this paper we also intend to compare the energetics of H_2O_2 (peroxidase activity) and $ONOO^-$/ONOOH (reductase activity) reduction by GPx and furthermore $ONOO^-$/ONOOH reduction by both ebselen and GPx.

COMPUTATIONAL DETAILS

(A) Adopted Models for the Enzyme and Substrates. Experimental studies on bovine erythrocyte GPx have suggested a half-site reactivity of the enzyme (*30*), which justifies the use of the active site of only a monomer to investigate the enzyme reactivity. Here, the first question to be considered is the choice of an appropriate model for the enzyme active site that retains all of its basic features. Since the selenocysteine residue is experimentally suggested to play a critical role in the catalytic cycle (*32*−*36*), it is included in the model. The active site Gln83 and Trp157 residues, known to be conserved in all known GPx's and experimentally suggested to be involved in the catalytic mechanism (*30*), are also included in the model. In addition, in the X-ray structure (*30*), Tyr48, Gly50, and Leu51 residues are shown to form a part of the cage around the selenocysteine residue; therefore, they are also included in the model. Since the active site of GPx has been suggested to contain water molecules (*42*), a water molecule is also included in the active site model. On the basis of the earlier experience glutamine and tryptophan residues are modeled by formamide and indole, respectively.

The next question to deal with is the active state of the enzyme. According to experiments, in the active state of the enzyme the selenocysteine residue could be either in selenolate anion (E−Se$^-$) or in selenol (E−SeH) form (*30*). In our previous study we justified the use of the selenol (E−SeH) as an active form of the enzyme (*39*). Depending on the nature of the substrate, i.e., either $ONOO^-$ or ONOOH, the overall charge of the model is chosen to be −1 or 0. The substrate GSH (γ-glutamylcysteinylglycine, γ-GluCysGly) is a tripeptide, which is modeled by ethanethiol (C_2H_5SH).

(B) Methods of Computation. All calculations were performed using the Gaussian 03 program (*43*). The geometries of reactants, intermediates, transition states, and products were optimized without any symmetry constraint using the B3LYP method (*44*) with the 6-31G(d) basis set. All degrees of freedom of proposed structures were optimized, and frequency calculations were performed for all optimized minima and transition states. It was confirmed that the calculated minima have no imaginary frequency, while all transition states have one imaginary frequency corresponding to the reaction coordinate. The final energetics of the optimized structures were improved by performing single point calculations using a triple-ζ quality basis set 6-311+G(d,p). Since it was computationally unfeasible to calculate zero-point energy and thermal corrections using the large basis set, these effects were estimated at the B3LYP/6-31G(d) level and added to the final B3LYP/6-311+G(d,p) energetics. This type of correction is an adequate approximation and has commonly been used in quantum chemical studies (*45*). The suggested mechanism of GPx involves peroxynitrite/peroxynitrous acid ($ONOO^-$/ONOOH) and a glutathione molecule, which consecutively enter the active site and participate in the catalytic reactions. Their exact binding sites prior to the participation in reactions are not known, and there is a large difference in the entropy contribution from the binding of an absolutely free and a prebonded molecule. Therefore, binding energies of these molecules without entropy contributions are more realistic than including entropy contributions without knowing their prereaction binding states. Since it is not possible to calculate reliable entropic contributions without knowing their prior binding states, they are assumed to be "free"; therefore, the entropy effects are not included in the final energetics.

The dielectric effects from the surrounding environment were estimated using the self-consistent reaction field IEF-PCM method (*46*) at the B3LYP/6-31G(d) level. These calculations were performed with a dielectric constant of 4.3 corresponding to diethyl ether, close to 4.0 generally used to describe the protein surrounding. Throughout the paper the energies obtained at the B3LYP/(6-311+G(d,p)) + zero-point energy (unscaled) and thermal corrections (at 298.15 K and 1 atm) + solvent effects [the last three terms at B3LYP/6-31G(d) level] are used, while the energies without the solvent effects are provided in parentheses.

RESULTS AND DISCUSSION

The suggested mechanism, shown in Figure 2, was used as a starting point for the present study. The overall reactions investigated in this study

$$ONOO^- + 2C_2H_5SH \rightarrow C_2H_5S{-}SC_2H_5 + NO_2^- + H_2O \quad \text{(A)}$$

$$ONOOH + 2C_2H_5SH \rightarrow C_2H_5S{-}SC_2H_5 + HNO_2 + H_2O \quad \text{(B)}$$

are calculated to be exothermic by 76.7 (69.9) and 66.4 (62.9) kcal/mol, respectively.

(A) Peroxynitrite/Peroxynitrous Acid ($ONOO^-$/ONOOH) Coordination. The coordination of substrate at the active site of the GPx enzyme is a first step of both oxidation and nitration pathways. The coordination of peroxynitrite ($ONOO^-$) to the active site of the enzyme (structure $\mathbf{I}_{0W}$, Figure 3) leads to the formation of structure $\mathbf{II}_P$ ($E{-}Se^-\cdots HO^1O^2NO^3\cdots H_2O$). $ONOO^-$ acts as a strong base, which abstracts a proton from the E−SeH upon binding to $\mathbf{I}_{0W}$. In $\mathbf{II}_P$, peroxynitrite interacts with the active site through hydrogen bonds with the water molecule, selenolate, and Gly50 residue. The binding energy of a free peroxynitrite to $\mathbf{I}_{0W}$ is calculated to be 19.6 (48.1) kcal/mol.

The protonated form of $ONOO^-$, peroxynitrous acid (ONOOH), binds at the active site of the enzyme (structure $\mathbf{I}_{0W}$, Figure 4) and forms a weakly interacting complex $E{-}Se{-}H\cdots H_2O\cdots HO^1O^2NO^3$ (structure $\mathbf{II}_{PA}$). The computed binding energy of free peroxynitrous acid is only 0.6 (6.5) kcal/mol. After the coordination of $ONOO^-$/ONOOH, the catalytic cycle proceeds through the oxidation and nitration pathways (see Figure 2), which are discussed separately.

(B) Oxidation Pathway. The first process occurring in this pathway is the formation of selenenic acid (E−Se−OH). The mechanism is quite different for the peroxynitrite and peroxynitrous acid substrates.

(1) Concerted Oxidation Mechanism for Peroxynitrite. The formation of the oxidation product (E−Se−OH) requires a hydroxyl group. For peroxynitrite ($ONOO^-$), the hydroxyl group required could be donated by either peroxynitrite (now in the form of HOONO in $\mathbf{II}_P$) or a water molecule located in the vicinity of the Se center. Since the source of the hydroxyl group is not known, both possibilities are explored in this study. In case the hydroxyl group is donated by peroxynitrite, the $O^1{-}O^2$ bond of the previously formed $E{-}Se^-\cdots HO^1O^2NO^3\cdots H_2O$ complex ($\mathbf{II}_P$) is broken and the hydroxyl group (O^1H) is concertedly transferred from the substrate to the selenolate ($E{-}Se^-$) ion to produce $ESe{-}O^1H$ ($\mathbf{III}_P$). The optimized structure of the corresponding transition state TS($\mathbf{II}_P{-}\mathbf{III}_P$) is shown in Figure 3. It is exothermic by 51.1 (49.9) kcal/mol and proceeds with a barrier of 4.7 (3.7) kcal/mol. The low barrier for $ONOO^-$ reduction is in agreement with the experimentally measured barrier of 8.8 kcal/mol for both GPx and ebselen (*29*) and the computed value of 7.1 kcal/mol for ebselen (*40*). The removal of a water molecule hydrogen-bonded to $ONOO^-$ from the model makes the peroxynitrite a stronger nucleophile and reduces the barrier by 2.6 (3.3) kcal/mol. However, it is worth mentioning that this process is most likely to occur in the presence of a water molecule as $ONOO^-$ binding does not remove the water molecule from the active site. The barrier associated with the donation of a hydroxyl group from the water molecule to the $E{-}Se^-$ is prohibitively high, ca. 40.0

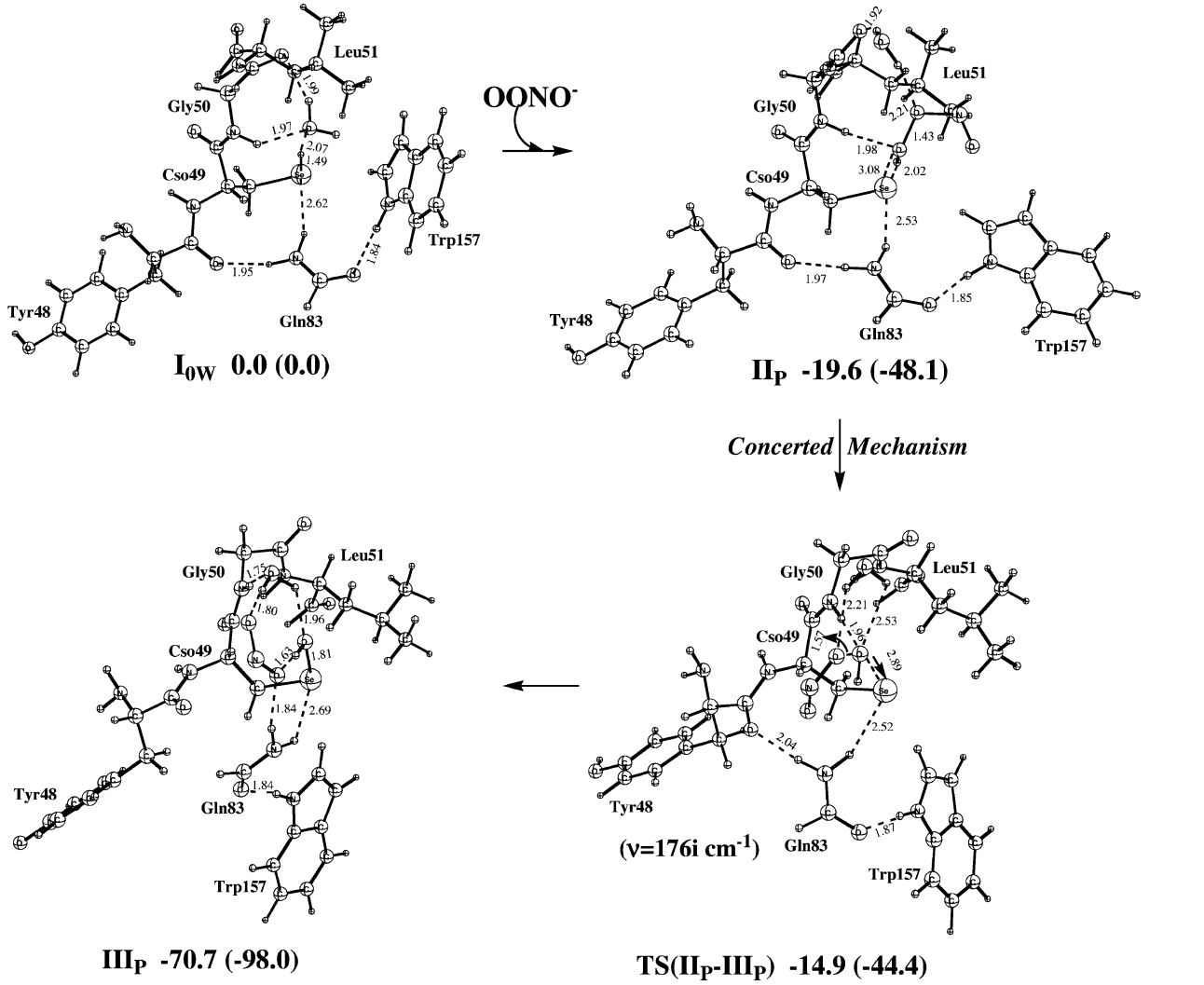

FIGURE 3: Optimized structures (distances in Å) and energies relative to the reactants [with and without (in parentheses) solvent effects, in kcal/mol] of intermediates and transition states in reaction 1 for the concerted oxidation mechanism using peroxynitrite ($ONOO^-$) as a substrate.

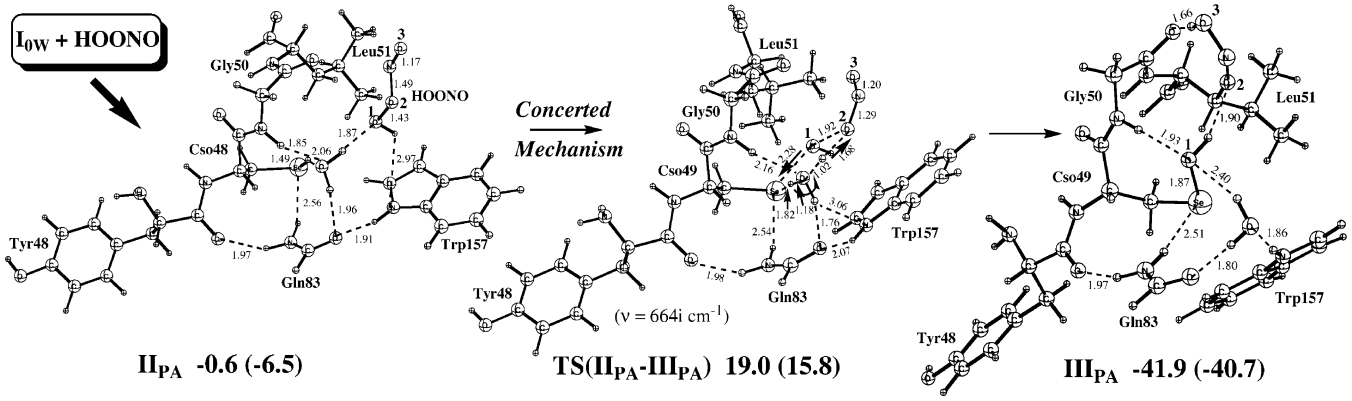

FIGURE 4: Optimized structures (distances in Å) and energies relative to the reactants [with and without (in parentheses) solvent effects, in kcal/mol] of intermediates and transition states in reaction 1 for the concerted oxidation mechanism using peroxynitrous acid (ONOOH) as a substrate.

kcal/mol (see transition state structure **TS1W** of the Supporting Information). These results explicitly indicate that the hydroxyl group required to produce the E−Se−OH is provided by peroxynitrite ($ONOO^-$) that is converted to ONOOH during its coordination. There is no stepwise mechanism corresponding to this step, as the O−O bond cleavage and hydroxyl group transfer are strongly coupled and cannot go through an intermediate.

(2) Concerted Oxidation Mechanism for Peroxynitrous Acid. For peroxynitrous acid (ONOOH), the E−Se−OH formation can take place via either a concerted or a stepwise mechanism. The stepwise mechanism consists of two parts:

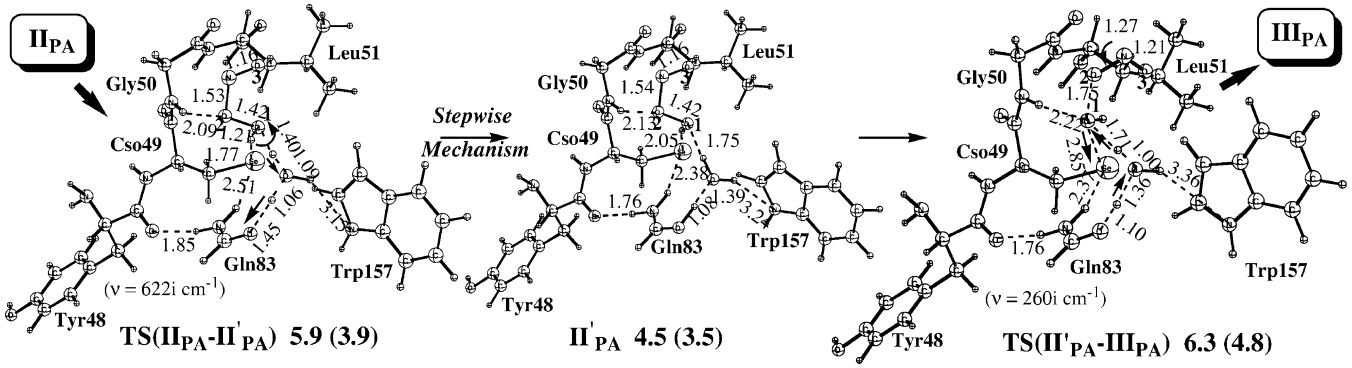

FIGURE 5: Optimized structures (distances in Å) and energies relative to the reactants [with and without (in parentheses) solvent effects, in kcal/mol] of intermediates and transition states in reaction 1 for the stepwise oxidation mechanism using peroxynitrous acid (ONOOH) as a substrate.

(a) formation of selenolate anion ($E-Se^-$) and (b) O−O bond cleavage. First, we discuss the concerted mechanism.

In the concerted mechanism for peroxynitrous acid ($O^3NO^2O^1H$), starting from the $\mathbf{II}_{PA}$ complex (Figure 4), the Se−H bond of the selenol (E−SeH) is broken, and with the help of a bridging water molecule a proton is transferred to $O^3NO^2O^1H$, which in turn facilitates the O^1-O^2 cleavage and subsequently the formation of the $ESe-O^1H$. The corresponding transition state **TS($\mathbf{II}_{PA}-\mathbf{III}_{PA}$)** is shown in Figure 4. The overall process $\mathbf{II}_{PA} \rightarrow \mathbf{III}_{PA}$ is exothermic by 41.3 (34.2) kcal/mol and proceeds with a 19.6 (22.3) kcal/mol barrier. In the absence of a water molecule in the model this barrier is further increased by 5.2 kcal/mol (in gas phase).

(3) Stepwise Oxidation Mechanism for Peroxynitrous Acid. In the first step of this mechanism, as shown in Figure 5, the Se−H bond of the selenol (E−SeH) is broken, and simultaneously the proton is transferred through the oxygen atom (O^1) of $O^3NO^2O^1H$ and a water molecule to the neighboring Gln83 producing the $\mathbf{II'}_{PA}$ intermediate involving the $E-Se^- + Gln83^+$ ion pair. The corresponding transition state, **TS($\mathbf{II}_{PA}-\mathbf{II'}_{PA}$)**, for this process is stabilized by hydrogen bonds with Gly50 and Trp157 residues. The $\mathbf{II}_{PA} \rightarrow \mathbf{II'}_{PA}$ process is found to be endothermic by 5.1 (10.0) kcal/mol and proceeds with a 6.5 (10.4) kcal/mol barrier from $\mathbf{II}_{PA}$. In $\mathbf{II'}_{PA}$ the O−H bond of 1.08 Å in $Gln83^+$ is slightly longer than the normal (0.98 Å) O−H bond. The absence of the water molecule in the model increases the barrier (by 6.4 kcal/mol in gas phase) and endothermicity (by 6.2 kcal/mol in gas phase) of the reaction.

In the second step of the stepwise pathway of the E−Se−OH formation, the O^1-O^2 bond of $O^3NO^2O^1H$ is cleaved, and the hydroxyl (O^1H) is transferred to the selenolate anion ($E-Se^-$). In this step, the proton previously transferred to the Gln83 residue moves to the oxygen atom (O^2) of $O^3NO^2O^1H$ and initiates the O^1-O^2 bond cleavage. As a result of this process, the $E-SeO^1H$ and HNO_2 (structure $\mathbf{III}_{PA}$) are produced. The transition state **TS($\mathbf{II'}_{PA}-\mathbf{III}_{PA}$)** indicates that this step is synchronous; i.e., all bond distances change smoothly from the intermediate $\mathbf{II'}_{PA}$ to the product $\mathbf{III}_{PA}$. The barrier for this process is only 1.8 (1.3) kcal/mol, which makes the overall barrier ($\mathbf{II}_{PA} \rightarrow \mathbf{III}_{PA}$) for the formation of the selenenic acid (E−Se−OH) 6.9 (11.3) kcal/mol. The presence of the water molecule significantly stabilizes the transition state as its removal from the model increases the barrier by 13.0 kcal/mol (in gas phase). This step of reaction 1 is calculated to be exothermic by 46.4 (44.2) kcal/mol. Since the overall barrier for the stepwise mechanism [6.9 (11.3) kcal/mol] is substantially lower than the barrier [19.6 (22.3) kcal/mol] for the concerted mechanism of the E−Se−OH formation, the latter mechanism is ruled out.

The aforementioned results explicitly indicate that the Gln83 residue plays a key role of a proton acceptor (step 1) and donor (step 2), which is consistent with the available experimental suggestion that the Gln83 residue participates in the catalytic cycle (*37*). Moreover, the water molecule located in the vicinity of the Se center also plays a very important role by directly participating in the reaction and reducing the barriers. In comparison to H_2O_2 reduction by GPx, where the calculated barrier for the enzyme oxidation through the identical stepwise mechanism is reported to be 17.1 (20.6) kcal/mol (see Figure 9), the overall barrier for ONOOH reduction by this enzyme is lower by 10.2 (9.3) kcal/mol. These results demonstrate that ONOOH is a more efficient substrate for the oxidation of selenocysteine than H_2O_2. On the other hand, in comparison to ebselen (a mimic of GPx), GPx catalyzes the reduction of ONOOH with a barrier higher by 3.9 kcal/mol (in gas phase) (*41*).

(4) Remaining Steps of the Oxidation Pathway. In this pathway, after the formation of selenenic acid (E−Se−OH), the remaining two steps (reactions 2 and 3) follow identical mechanisms as suggested for H_2O_2 reduction by GPx in our previous computational study (*39*). Therefore, these two steps are not discussed in detail here, and only their energetics are reported in brief. In reaction 2, the E−Se−OH reacts with the first molecule of the substrate glutathione (GSH) to form the E−Se−SG adduct, which has been observed experimentally (*36*). This reaction occurs with a barrier of 17.9 (22.6) kcal/mol and is exothermic by 15.9 (23.4) kcal/mol (*39*). In the third and rate-limiting step (reaction 3) of the catalytic cycle, the E−Se−SG adduct reacts with the second molecule of GSH to form the oxidized form of glutathione, $C_2H_5S-SC_2H_5$, and the enzyme returns back to its original form. Reaction 3 is found to be exothermic by 3.9 (15.2) kcal/mol and occurs with a barrier of 21.5 (25.5) kcal/mol (*39*).

(C) Nitration Pathways. This pathway, after the binding of $ONOO^-$/ONOOH to the active site (structure $\mathbf{II}_{PA}$, Figure 6), leads to the nitration of the selenol (E−Se−H). In general, the nitration product $E-Se-NO_2$ can exist in two different

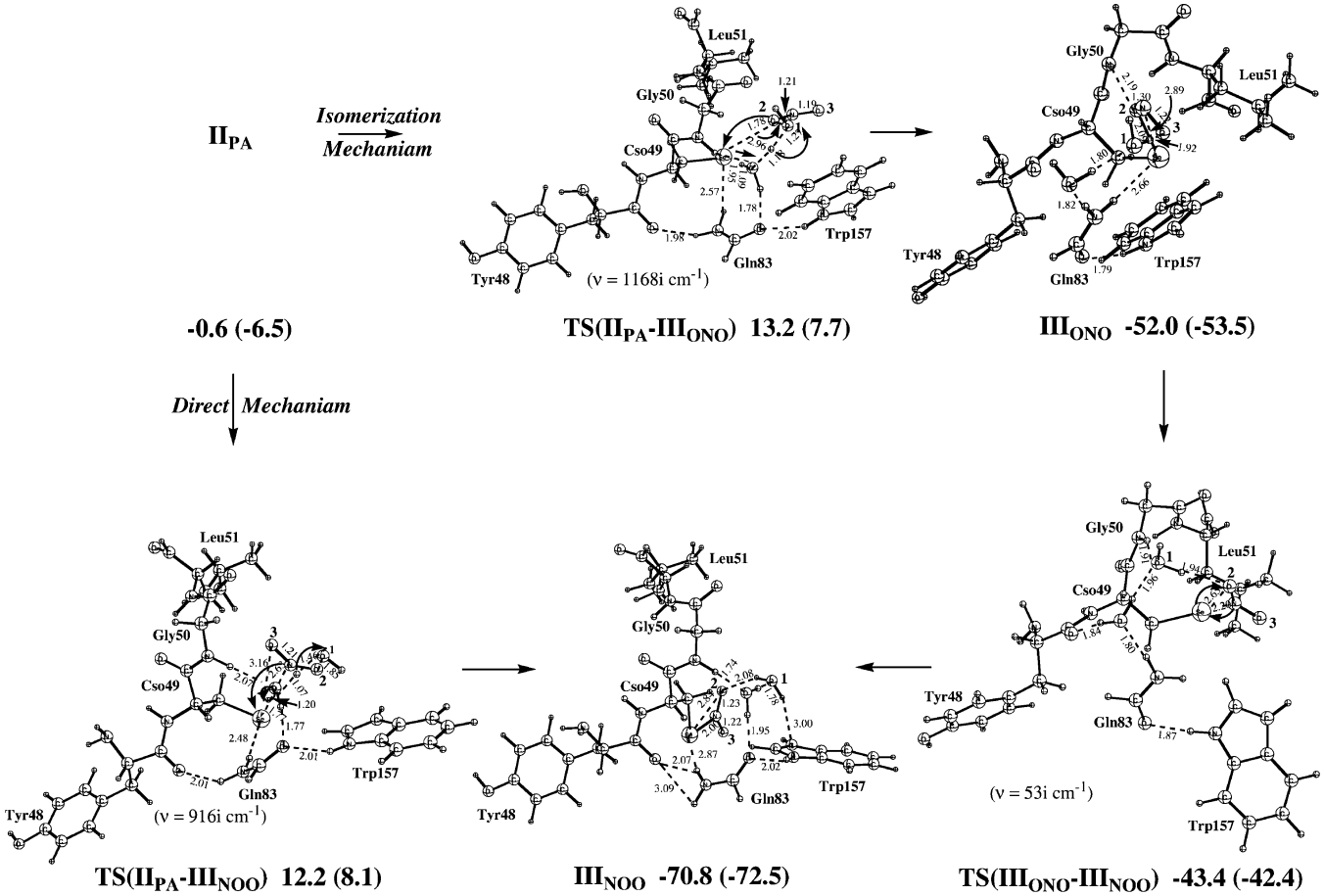

FIGURE 6: Optimized structures (distances in Å) and energies relative to the reactants [with and without (in parentheses) solvent effects, in kcal/mol] of intermediates and transition states in reaction 1 for the isomerization and direct mechanisms in the nitration pathway using peroxynitrous acid (ONOOH) as a substrate.

isomeric forms, nitro (E−Se−NOO) and nitrito (E−Se−O−N═O), which can be formed by the reactions of both peroxynitrite ($ONOO^-$) and peroxynitrous acid (ONOOH) with the active site selenocysteine residue. However, the use of $ONOO^-$ creates a highly reactive hydroxyl (OH^-) ion which could readily react with the active site amino acid residues. The enzyme may be set up to control these ions, but this unknown regulation process is hard to model. Therefore, to avoid these side reactions, in this study, the nitration pathway is investigated only for the HNOOH substrate. The B3LYP calculations suggest that the formation of the E−Se−NOO (structure $\mathbf{III}_{NOO}$) is thermodynamically 18.8 (19.0**)** kcal/mol more favorable than the E−Se−O−N═O (structure $\mathbf{III}_{ONO}$) and can occur through the following two mechanisms: (1) isomerization mechanism and (2) direct mechanism. In the former, the first $\mathbf{III}_{ONO}$ species is generated which then isomerizes to the energetically more favorable product $\mathbf{III}_{NOO}$, whereas in the latter $\mathbf{III}_{NOO}$ is generated directly.

(1) Isomerization Mechanism. In the first part of this mechanism, the Se−H bond of the selenol (E−SeH), $\mathbf{II}_{PA}$, is broken, and with the help of the bridging water molecule a proton is transferred to the terminal oxygen atom (O^1) of $O^3NO^2O^1H$, which facilitates the O^1-O^2 bond cleavage and leads to the formation of the $E-Se-O^3-N{=}O^2$ ($\mathbf{III}_{ONO}$) and a water molecule. The optimized transition state for this process, structure **TS(**$\mathbf{II}_{PA}-\mathbf{III}_{ONO}$**)** is shown in Figure 6. The computed barrier for the formation of $\mathbf{III}_{ONO}$ is 13.8 (14.2) kcal/mol, which could be slightly overestimated because the B3LYP method is known to overestimate the activation energy for long-range proton transfer reaction (*47*). The formation of this intermediate is exothermic by 51.4 (47.0) kcal/mol. Similar to the oxidation pathway, here also the water molecule plays a key role in the mechanism by keeping the barrier low. It was found that the removal of the water molecule from the model increases the barrier for this process by 7.2 kcal/mol (in gas phase).

A stepwise mechanism, similar to the one (involving Gln83) investigated for the formation of $\mathbf{III}_{PA}$ in the oxidation pathway, was also investigated for the generation of $\mathbf{III}_{ONO}$. However, all of the attempts to locate the transition state for the O^1-O^2 bond splitting of $O^3NO^2O^1H$ failed as its optimization always leads to the above-discussed concerted mechanism. On the basis of this result it can be concluded that the stepwise mechanism for the formation of the E−Se−O−N═O product does not exist.

In the second part of this isomerization mechanism, the formed $\mathbf{III}_{ONO}$ isomerizes to $\mathbf{III}_{NOO}$. During this isomerization, the $Se-O^2$ bond of $\mathbf{III}_{ONO}$ is broken, and the Se−N bond is formed. In the associated transition state **TS(**$\mathbf{III}_{ONO}-\mathbf{III}_{NOO}$**)**, the $Se-O^2$ and Se−N bond distances of 2.65 and 2.20 Å, respectively, are between the corresponding distances in $\mathbf{III}_{ONO}$ (2.09 and 2.89 Å) and $\mathbf{III}_{NOO}$ (2.84 and 2.00 Å), which clearly indicate the transformation of the intermediate E−Se−O−N═O to the E−Se−NOO. The $\mathbf{III}_{ONO} \rightarrow \mathbf{III}_{NOO}$ isomerization is found to be exothermic

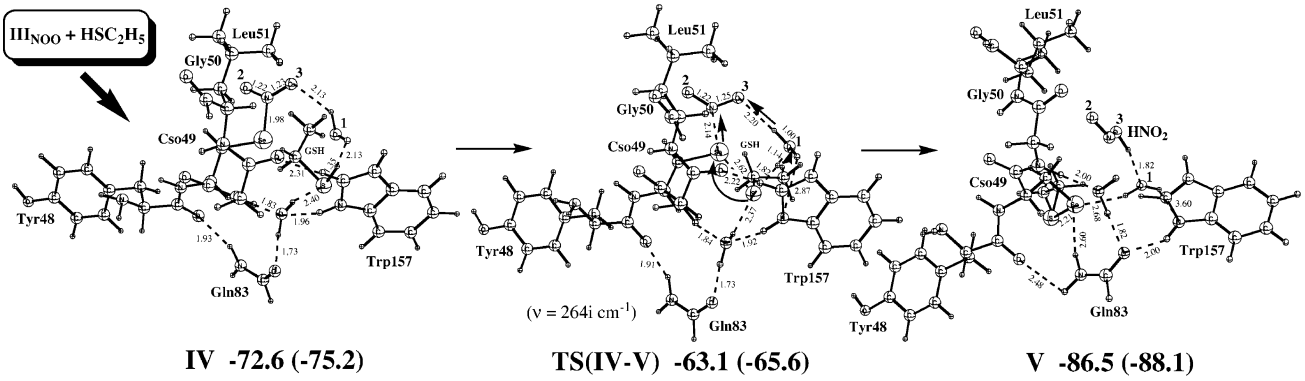

FIGURE 7: Optimized structures (distances in Å) and energies relative to the reactants [with and without (in parentheses) solvent effects, in kcal/mol] of intermediates and transition states in reaction 2 for the nitration pathway using peroxynitrous acid (ONOOH) as a substrate.

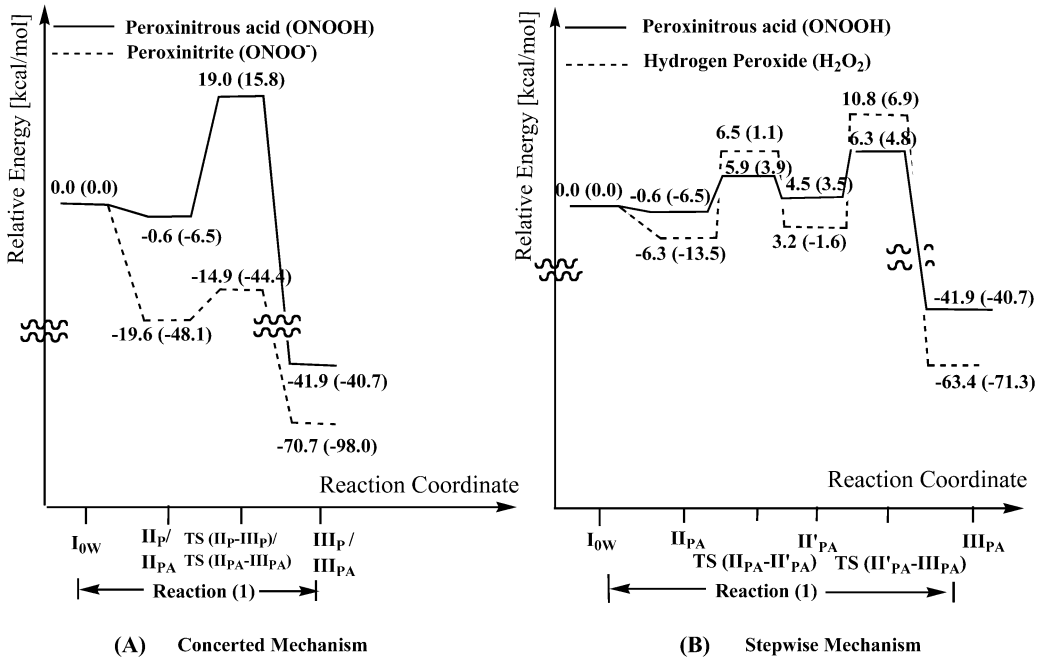

FIGURE 8: Energy diagram for reaction 1 of the oxidation pathway [with and without (in parentheses) solvent effects, in kcal/mol]. The energy scale is set up for the values including solvent effects.

by 18.8 (19.0) kcal/mol and proceeds with a barrier of 8.6 (11.1) kcal/mol.

(2) Direct Mechanism. In this mechanism, in **II**$_{PA}$ the Se−H bond of the selenol (E−SeH) is broken, and with the help of a bridging water molecule a proton is transferred to the terminal oxygen atom (O^1) of $O^3NO^2O^1H$, which in turn cleaves the O^1-O^2 bond and produces the $E-Se-NO^2O^3$ (**III**$_{NOO}$) species and a water molecule (H_2O^1). In the corresponding transition state **TS(II**$_{PA}$**−III**$_{NOO}$**)** shown in Figure 7, the Se−N and $Se-O^2$ bond distances of 2.63 and 3.16 Å, respectively, clearly indicate the formation of **III**$_{NOO}$. The barrier for this concerted mechanism is 12.8 (14.6) kcal/mol, and this process is exothermic by 70.2 (66.0) kcal/mol. In this process also a long-range proton transfer takes place, which could be slightly overestimated by the B3LYP method (*47*). Since for the generation of **III**$_{ONO}$ the exclusion of a water molecule in the model raises the barrier by 7.2 kcal/mol (in gas-phase), this possibility is not explored here. As discussed above for the formation of **III**$_{ONO}$, the stepwise mechanism involving the Gln83 residue does not exist in the direct generation of **III**$_{NOO}$ as well.

The calculated barriers for the nitration of the selenocysteine by peroxynitrous acid through the isomerization and direct mechanisms, 13.8 (14.2) and 12.8 (14.6) kcal/mol, are very close. While the direct mechanism is slightly preferred, the accuracy of the methods applied in this study does not allow a clear discrimination between these two mechanisms. Therefore, it can be concluded that both of these mechanisms for the selenocysteine nitration by ONOOH are plausible.

(3) Reaction of the Nitro Product (E−Se−NOO) with Glutathione (GSH). Reaction 2 of the nitration pathway (see Figure 2) starts with the coordination of the first unbound glutathione molecule to **III**$_{NOO}$ and leads to the formation of a weakly bound ($E-SeNO^2O^3$)- - -(GSH) complex **IV** (Figure 7) with the binding energy of 1.8 (2.7) kcal/mol. From **IV** the reaction proceeds through the transition state **TS(IV−V)** and produces the seleno−sulfide (E−Se−S−G) adduct and HNO_2 (structure **V**). As shown in Figure 7, at the transition state **TS(IV−V)**, synchronously the S−H bond of glutathione is broken, and through the water molecule a proton is transferred to O^3 of the $E-Se-NO^3O^2$

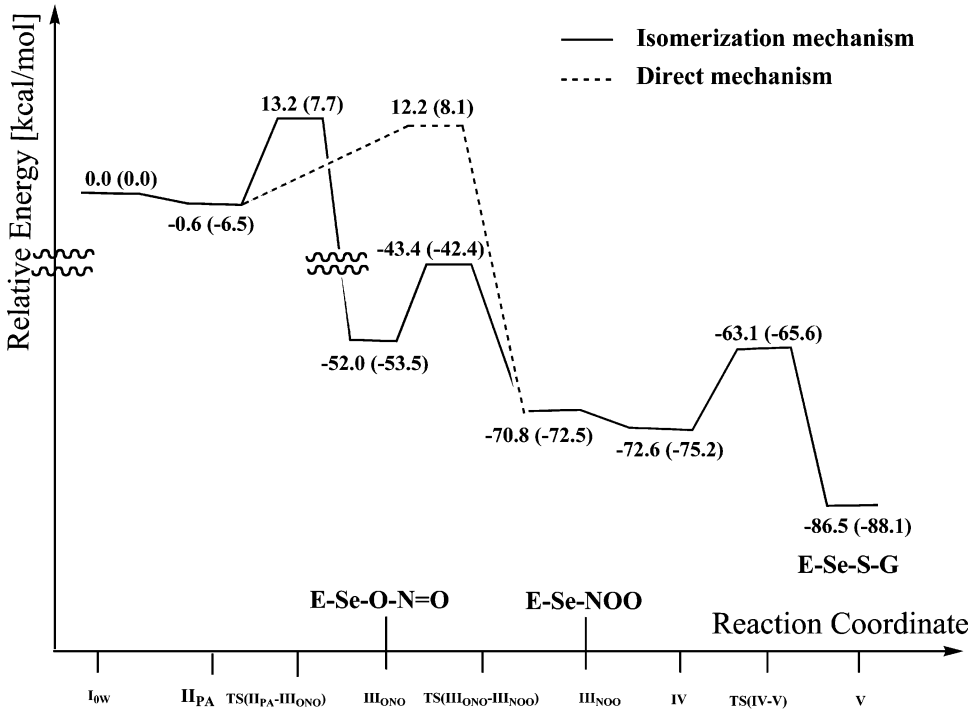

FIGURE 9: Energy diagram for reactions 1 and 2 of the nitration pathway [with and without (in parentheses) solvent effects, in kcal/mol]. The energy scale is set up for the values including solvent effects.

accompanied by the formations of a Se−S bond and nitrous acid (HNO_2). The barrier for this step is calculated to be 9.5 (9.6) kcal/mol, and it is exothermic by 13.9 (12.9) kcal/mol.

Also in this reaction, the water molecule plays a critical role by significantly reducing the barrier by 15.7 kcal/mol (in gas phase). This large effect could be explained by comparing the TS structures with and without the participation of the water molecule. In **TS(IV−V)**, the Se−S and Se−N distances are considerably shorter (0.14 and 0.62 Å, respectively) than the corresponding distances without the water molecule. Moreover, the direct participation of the water molecule also provides an additional hydrogen bond. In the presence of a water molecule **TS(IV−V)** appears to be optimum for the formation of the Se−S bond.

In a similar way, $\mathbf{III}_{ONO}$ is also found to react with the substrate GSH to produce the seleno−sulfide (E−Se−S−G) adduct and HNO_2. As shown in the Supporting Information, first a molecule of GSH binds to $\mathbf{III}_{ONO}$ to form a ($E-Se-O^3-N=O^2$)- - -(GSH) complex (structure $\mathbf{IV}_{ONO}$) with the binding energy of 1.8 (2.7) kcal/mol, which then rearranges to **V** through $\mathbf{TS(IV}_{ONO}\mathbf{-V)}$ with a small barrier of 1.3 (1.0) kcal/mol.

After the formation of the E−Se−S−G adduct, the third and final step, reaction 3, of the overall mechanism is identical in both oxidation and nitration mechanisms, which was already discussed above.

OVERALL REACTION MECHANISMS AND CONCLUSIONS

The overall potential energy diagrams for the concerted and stepwise mechanisms of the oxidation pathway are shown in Figure 8. The oxidation of GPx with peroxynitrite ($ONOO^-$) can occur only via a concerted mechanism. It involves the coordination of $ONOO^-$ to the active site and the subsequent formation of the selenenic acid (E−Se−OH) with only a 4.7 (3.7) kcal/mol barrier. The overall process is highly exothermic by 70.7 (98.0) kcal/mol. The calculated barrier is in good agreement with the computed barrier of 7.1 kcal/mol for ebselen (*40*) and the experimentally measured barrier of 8.8 kcal/mol for both GPx and ebselen (*29*).

However, the oxidation of the selenocysteine by peroxynitrous acid ONOOH via the similar concerted mechanism is less favorable, by 12.7 (11.0) kcal/mol, than the stepwise mechanism which involves the following two steps: (a) formation of selenolate anion ($E-Se^-$) and (b) O−O bond cleavage. In the first step, a proton transfer from the E−Se−H through an active site water molecule to the neighboring Gln83 residue occurs with a barrier of 6.5 (10.4) kcal/mol and leads to the intermediate $\mathbf{II'}_{PA}$ involving the $E-Se^- + Gln83^+$ ion pair. This step of the reaction is calculated to be endothermic by 5.1 (10.0) kcal/mol. In the second step, the proton previously transferred to $Gln83^+$ migrates to the ONOOH fragment and leads to the formation of E−Se−OH and HNO_2 products ($\mathbf{III}_{PA}$). It occurs with a 1.8 (1.3) kcal/mol barrier and is exothermic by 46.4 (44.2) kcal/mol. As shown in the energy diagram (Figure 8B), the entire process $\mathbf{I}_{0W} + ONOOH \rightarrow E-Se-OH + HNO_2$ is highly exothermic by 41.9 (40.7) kcal/mol and proceeds with an overall energy barrier of 6.9 (11.3) kcal/mol.

The results presented in this study clearly demonstrate that the water molecule in the vicinity of the active site and the Gln83 residue play a crucial role by explicitly participating in the oxidation reaction. The comparison of the energetics of the reaction ($\mathbf{I}_{0W} + ONOOH \rightarrow E-Se-OH + HNO_2$) with the previously investigated one ($\mathbf{I}_{0W} + HOOH \rightarrow E-Se-OH + H_2O$, also shown in Figure 8B) shows that the overall barrier for GPx oxidation by ONOOH is lower by 10.2 (11.2) kcal/mol (*39*). This result indicates that peroxynitrous acid (ONOOH) is a more efficient substrate for the oxidation of GPx than hydrogen peroxide (H_2O_2).

The nitration pathway was studied only for the ONOOH substrate. Since the $ONOO^-$ substrate generates a highly reactive OH^- ion, we believe that there must be a mechanism that controls the formation of this ion. It was found that a nitro product (E−Se−NOO), $\mathbf{III}_{NOO}$, is thermodynamically most favorable. The overall potential energy profiles for two mechanisms to produce the nitro product, (1) isomerization mechanism and (2) direct mechanism, are shown in Figure 9. The formation of $\mathbf{III}_{NOO}$ through the successive generation and isomerization of the intermediate $\mathbf{III}_{ONO}$ (isomerization mechanism) is slightly less favorable than the direct formation of $\mathbf{III}_{NOO}$, with the calculated barriers of 13.8 (14.2) and 12.8 (14.6) kcal/mol, respectively. The accuracy of the methods employed does not allow discrimination between these two mechanisms with such a small difference in barriers. Therefore, we conclude that both of these mechanisms of selenocysteine nitration by ONOOH are equally feasible. The nitration reaction E−SeH + ONOOH → E−Se−NOO + H_2O is found to be exothermic by 70.2 (66.0) kcal/mol. A comparison of the calculated rate-determining barriers of 6.9 (11.3) and 12.8 (14.6) kcal/mol for the oxidation and nitration, respectively, of the selenocysteine by ONOOH indicates that the formation of the E−SeOH (the oxidation product) is much more preferable.

In reaction 2, the coordination of the first unbound GSH to the oxidation (E−SeOH) and nitration [E−Se−NOO ($\mathbf{III}_{NOO}$)] products forms weakly bound E−SeOH- - -GSH and E−SeNOO- - -GSH (**IV**) intermediates, which eventually transforms to the E−Se−S−G + H_2O and E−Se−S−G + HNO_2 (**V**) products with barriers of 17.9 (22.6) and 9.5 (9.6) kcal/mol, respectively. After the formation of the E−Se−S−G adduct, in the final reaction (E−Se−S−G + GSH → E−Se−H + GS−SG), the oxidized form of glutathione ($C_2H_5S-SC_2H_5$) is generated, and the enzyme returns back to its original form. In our previous study, it was shown that this reaction occurs with a 21.5 (25.5) kcal/mol barrier (*39*), which makes it rate-limiting for both peroxidase and peroxynitrite/peroxynitrous reductase activity of GPx. Therefore, it can be concluded that for both H_2O_2 peroxidase and $ONOO^-$/ONOOH reductase (irrespective of the pathway followed) activities of the GPx enzyme the rate-determining barrier remains the same.

The results reported in this study shed light on the existence of two different (oxidation and nitration) pathways, substrate specificities, and the important role played by the active site water molecule and the Gln83 residue, as well as the details of the every step in the catalysis which will enhance our understanding of the complex functioning of this critical enzyme.

ACKNOWLEDGMENT

A DURIP grant (FA9550-04-1-0321) from AFOSR is acknowledged for support of the computer facilities. The use of computational resources at the Cherry Emerson Center for Scientific Computation is also acknowledged.

SUPPORTING INFORMATION AVAILABLE

(a) Complete ref *43*; (b) Tables S1−S5, Cartesian coordinates (in Å) of all the optimized structures including transition states in reaction 1 for the concerted oxidation mechanism using peroxynitrite ($ONOO^-$) as a substrate; (c) Tables S6−S8, Cartesian coordinates (in Å) of all the optimized structures including transition states in reaction 1 for the concerted oxidation mechanism using peroxynitrous acid (ONOOH) as a substrate; (d) Tables S9−S11, Cartesian coordinates (in Å) of all the optimized structures including transition states in reaction 1 for the stepwise oxidation mechanism using peroxynitrous acid (ONOOH) as a substrate; (e) Tables S12−S16, Cartesian coordinates (in Å) of all the optimized structures including transition states in reaction 1 for the isomerization and direct mechanisms in the nitration pathway using peroxynitrous acid (ONOOH) as a substrate; and (f) Tables S17−S21, Cartesian coordinates (in Å) of all the optimized structures including transition states in reaction 2 for the nitration pathway using peroxynitrous acid (ONOOH) as a substrate. This material is available free of charge via the Internet at http://pubs.acs.org.

REFERENCES

1. Mills, G. C. (1957) Hemoglobin catabolism. I. Glutathione peroxidase, an erythrocyte enzyme which protects hemoglobin from oxidative breakdown, *J. Biol. Chem. 229*, 189−197.
2. Flohè, L. (1989) *Glutathione* (Dolphin, D., Avramovic, O., and Poulson, R., Eds.) pp 644−731, John Wiley & Sons, New York.
3. Sies, H., Sharov, V. S., Klotz, L. O., and Briviba, K. (1997) Glutathione peroxidase protects against peroxinitrite-mediated oxidations: a new function for selenoproteins as peroxynitrite reductase, *J. Biol. Chem. 272*, 27812−27817.
4. Birringer, M., Pilawa, S., and Flohè, L. (2002) Trends in selenium Chemistry, *Nat. Prod. Rep. 19*, 693−718.
5. (a) Beckman, J. S., and Crow, J. P. (1993) Pathological implications of nitric oxide, superoxide and peroxynitrite formation, *Biochem. Soc. Trans. 21*, 330−334; (b) Ischiropoulos, H., Zhu, L., and Beckman, J. S. (1992) Peroxynitrite formation from macrophage-derived nitric oxide, *Arch. Biochem. Biophys. 298*, 446−451; (c) Huie, R. E., and Padmaja, S. (1993) The reaction of nitric oxide with superoxide, *Free Radical Res. Commun. 18*, 195−199.
6. Beckman, J. S., Beckman, T. W., Chen, J., Marshall, P. A., and Freeman, B. A. (1990) Apparent hydroxyl radical production by peroxynitrite: implications for endothelial injury from nitric oxide and superoxide *Proc. Natl. Acad. Sci. U.S.A. 87*, 1620−1624.
7. Koppenol, W. H., Moreno, J. J., Pryor, W. A., Ischiropoulos, H., and Beckman, J. S. (1992) Peroxynitrite, a cloaked oxidant formed by nitric oxide and superoxide, *Chem. Res. Toxicol. 5*, 834−842.
8. Pryor, W. A., Gueto, R., Jin, X., Koppenol, W. H., Ngu-Schwemlein, M., Squadrito, G. L., Uppu, P. L., and Uppu, R. M. (1995) A practical method for preparing peroxynitrite solutions of low ionic strength and free of hydrogen peroxide, *Free Radical Biol. Med. 18*, 75−83.
9. Uppu, R. M., Squadrito, G. L., and Pryor, W. A. (1996) Acceleration of peroxynitrite oxidations by carbon dioxide, *Arch. Biochem. Biophys. 327*, 335−343.
10. (a) Lymar, S. V., and Hurst, J. K. (1998) Radical nature of peroxynitrite reactivity, *Chem. Res. Toxicol. 11*, 714−715; (b) Lymar, S. V., Jiang, Q., and Hurst, J. K. (1996) Mechanism of carbon dioxide-catalyzed oxidation of tyrosine by peroxynitrite, *Biochemistry 35*, 7855−7891.
11. Goldstein, S., and Czapski, G. (1998) Formation of peroxynitrate from the reaction of peroxynitrite with CO_2: Evidence for carbonate radical production, *J. Am. Chem. Soc. 120*, 3458−3463.
12. Rosen, G. M., and Freeman, B. A. (1984) Detection of superoxide generated by endothelial cells, *Proc. Natl. Acad. Sci. U.S.A. 81*, 7269−7273.
13. Marla, S. S., Lee, J., and Groves, J. T. (1997) Peroxynitrite rapidly permeates phospholipid membranes, *Proc. Natl. Acad. Sci. U.S.A. 94*, 14243−14248.
14. Denicola, A., Souza, J. M., and Radi, R. (1998) Diffusion of peroxynitrite across erythrocyte membranes, *Proc. Natl. Acad. Sci. U.S.A. 95*, 3566−3571.
15. Rachmilewitz, D., Stamler, J. S., Karmeli, F., Mullins, M. E., Singel, D. J., Loscalzo, J., Xavier, R. J., and Podolsky, D. K. (1993) Peroxynitrite-induced rat colitis—a new model of colonic inflammation, *Gastroenterology 105*, 1681−1688.

16. Squadrito, G. L., Jin, X., and Pryor, W. A. (1995) Stopped-flow kinetic study of the reaction of ascorbic acid with peroxynitrite, *Arch. Biochem. Biophys. 322*, 53−59.
17. Lee, J., Hunt, J. A., and Groves, J. T. (1998) Manganese porphyrins as redox-coupled peroxynitrite reductases, *J. Am. Chem. Soc. 120*, 6053−6061.
18. Crow, J. P., Beckman, J. S., and McCord, J. M. (1995) Sensitivity of the essential zinc-thiolate moiety of yeast alcohol dehydrogenase to hypochlorite and peroxynitrite, *Biochemistry 43*, 3544−3552.
19. Gatti, R. M., Radi, R., and Augusto, O. (1994) Peroxynitrite-mediated oxidation of albumin to the protein-thiyl free radical, *FEBS Lett. 348*, 287−290.
20. Szabo, C., and Ohshima, H. (1997) DNA damage induced by peroxynitrite: subsequent biological effects, *Nitric Oxide: Biol. Chem. 1*, 373−385.
21. Burk, R. F., Ed. (1994) *Selenium in Biology and Human Health*, Springer-Verlag, New York.
22. (a) Floris, R., Piersma, S. R., Yang, G., Jones, P., and Wever, R. (1993) Interaction of myeloperoxidase with peroxynitrite. A comparison with lactoperoxidase, horseradish peroxidase and catalase, *Eur. J. Biochem. 215*, 767−775; (b) Kondo, H., Takahashi, M., and Niki, E. (1997) Peroxynitrite-induced hemolysis of human erythrocytes and its inhibition by antioxidants, *FEBS Lett. 413*, 236−238; (c) Exner, M., and Herold, S. (2000) Kinetic and mechanistic studies of the peroxynitrite-mediated oxidation of oxymyoglobin and oxyhemoglobin, *Chem. Res. Toxicol. 13*, 287−293; (d) Squadrito, G. L., and Pryor, W. A. (1998) The nature of reactive species in systems that produce peroxynitrite, *Chem. Res. Toxicol. 11*, 718−719; (e) Radi, R. (1998) Nitric oxide and peroxynitrite-dependent aconitase inactivation and iron-regulatory protein-1 activation in mammalian fibroblasts, *Chem. Res. Toxicol. 11*, 720−721; (f) Minetti, M., Scorza, G., and Pietraforte, D. (1999) Peroxynitrite induces long-lived tyrosyl radical(s) in oxyhemoglobin of red blood cells through a reaction involving CO_2 and a ferryl species, *Biochemistry 38*, 2078−2087; (g) Herold, S., Matsui, T., and Watanabe, Y. (2001) Peroxynitrite isomerization catalyzed by his64 myoglobin mutants, *J. Am. Chem. Soc. 123*, 4085−4086; (h) Bourassa, J. L., Ives, E. P., Marqueling, A. L., Shimanovich, R., and Groves, J. T. (2001) Myoglobin catalyzes its own nitration, *J. Am. Chem. Soc. 123*, 5142−5143.
23. (a) Stern, M. K., Jensen, M. P., and Kramer, K. (1996) Peroxynitrite decomposition catalysts, *J. Am. Chem. Soc. 118*, 8735−8736; (b) Crow, J. P. (1999) Manganese and iron porphyrins catalyze peroxynitrite decomposition and simultaneously increase nitration and oxidant yield: implications for their use as peroxynitrite scavengers in vivo, *Arch. Biochem. Biophys. 371*, 41−52; (c) Hunt, J. A., Lee, J., and Groves, J. T. (1997) Amphiphilic peroxynitrite decomposition catalysts in liposomal assemblies, *Chem. Biol. 4*, 845−858; (d) Crow, J. P. (2000) Peroxynitrite scavenging by metalloporphyrins and thiolates, *Free Radical Biol. Med. 28*, 1487−1494; (e) Balavoine, G. G. A., Geletti, Y. V., and Bejan, D. (1997) *Nitric Oxide: Biol. Chem. 1*, 507; (f) Shimanovich, R., Hannah, S., Lynch, V., Gerasimchuk, N., Mody, T. D., Magda, D., Sessler, J., and Groves, J. T. (2001) Mn(II)-texaphyrin as a catalyst for the decomposition of peroxynitrite, *J. Am. Chem. Soc. 123*, 3613−3614; (g) Zhang, X., and Busch, D. H. (2000) Mn(II)-texaphyrin as a catalyst for the decomposition of peroxynitrite, *J. Am. Chem. Soc. 122*, 1229−1230; (h) Salvemini, D., Wang, Z. Q., Stern, M., Currie, M. G., and Misko, T. (1998) Peroxynitrite decomposition catalysts: therapeutics for peroxynitrite-mediated pathology, *Proc. Natl. Acad. Sci. U.S.A. 95*, 2659−2663.
24. (a) Mugesh, G., and Singh, H. B. (2000) Synthetic organoselenium compounds as antioxidant: glutathione peroxidase activity, *Chem. Soc. Rev. 29*, 347−357; (b) Mugesh, G., Panda, A., Singh, H. B., Punekar, N. S., and Butcher, R. J. (2001) Glutathione peroxidase-like antioxidant activity of diaryl diselenides: A mechanistic study, *J. Am. Chem. Soc. 123*, 839−850; (c) Mugesh, G., du Mont, W. W., and Sies, H. (2001) Chemistry of biologically important synthetic organoselenium compounds, *Chem. Rev. 101*, 2125−2179; (d) Briviba, K., Roussyn, I., Sharov, V. S., and Sies, H. (1996) Attenuation of oxidation and nitration reactions of peroxynitrite by selenomethionine, selenocystine and ebselen, *Biochem. J. 319*, 13−15.
25. (a) Cadenas, E., Wefers, H., Muller, A., Brigelius, R., and Sies, H. (1982) in *Agents and Actions Supplements* (Parnham, M. J., and Winkelmann, J., Eds.) Vol. 11, p 203, Birkhauser-Verlag-Basel; (b) Parnham, M. J., Leyck, S., Kuhl, P., Schalkwijk, J., and Van den Berg, W. B. (1987) Ebselen: a new approach to the inhibition of peroxide-dependent inflammation, *Int. J. Tissue React. 9*, 45−50; (c) Wendel, A., and Tiegs, G. (1986) A novel biologically active seleno-organic compound—VI. Protection by ebselen (PZ 51) against galactosamine/endotoxin-induced hepatitis in mice, *Biochem. Pharmacol. 35*, 2115−2118; (d) Kuhl, P., Borbe, H. O., Fischer, H., Romer, A., and Safayhi, H. (1986) Ebselen reduces the formation of LTB4 in human and porcine leukocytes by isomerisation to its 5S,12R-6-trans-isomer, *Prostaglandins 31*, 1029−1048; (e) Parnham, M. J., and Graf, E. (1987) Seleno-organic compounds and the therapy of hydroperoxide-linked pathological conditions, *Biochem. Pharmacol. 36*, 3095−3102.
26. Masumoto, H., Kissner, R., Koppenol, W. H., and Sies, H. (1996) Kinetic study of the reaction of ebselen with peroxynitrite, *FEBS Lett. 398*, 179−182.
27. Sies, H., and Masumoto, H. (1997) *Adv. Pharmacol. 38*, 229.
28. Perrin, D., and Koppenel, W. H. (2000) The quantitative oxidation of methionine to methionine sulfoxide by peroxynitrite, *Arch. Biochem. Biophys. 377*, 266−272.
29. Briviba, K., Kissner, R., Koppenol, W. H., and Sies, H. (1998) Kinetic study of the reaction of glutathione peroxidase with peroxnitrite, *Chem. Res. Toxicol. 11*, 1398−1401.
30. Epp, O., Ladenstein, R., and Wendel, A. (1983) The refined structure of the selenoenzyme glutathione peroxidase at 0.2-nm resolution, *Eur. J. Biochem. 133*, 51−69.
31. Ren, B., Huang, W., Åkesson, B., and Ladenstein, R. (1997) The crystal structure of seleno-glutathione peroxidase from human plasma at 2.9 Å resolution, *J. Mol. Biol. 268*, 869−885.
32. Prohaska, J. R., Oh, S. H., Hoekstra, W. G., and Ganther, H. E. (1977) Glutathione peroxidase: inhibition by cyanide and release of selenium, *Biochem. Biophys. Res. Commun. 74*, 64−71.
33. Forstrom, J. W., Zakowski, J. J., and Tappel, A. L. (1978) Identification of the catalytic site of rat liver glutathione peroxidase as selenocysteine, *Biochemistry 17*, 2639−2644.
34. Wendel, A., Pilz, W., Ladenstein, R., Sawatzki, G., and Weser, U. (1975) Substrate-induced redox change of selenium in glutathione peroxidase studied by X-ray photoelectron spectroscopy, *Biochim. Biophys. Acta 377*, 211−215.
35. Ladenstein, R., Epp, O., Bartels, K., Jones, A., Huber, R., and Wendel, A. (1979) Structure analysis and molecular model of the selenoenzyme glutathione peroxidase at 2.8 Å resolution, *J. Mol. Biol. 134*, 199−218.
36. Kraus, R. J., and Ganther, H. E. (1980) Reaction of cyanide with glutathione peroxidase, *Biochem. Biophys. Res. Commun. 96*, 1116−1122.
37. Ursini, F., Maiorino, M., Brigelius-Flohé, R., Aumann, K. D., Roveri, A., Schomburg, D., and Flohé, L. (1995) Diversity of glutathione peroxidases, *Methods Enzymol. 252*, 38−53.
38. Padmaja, S., Squadrito, G. L., and Pryor, W. A. (1998) Inactivation of glutathione peroxidase by peroxinitrite, *Arch. Biochem. Biophys. 349*, 1−6.
39. Prabhakar, R., Vreven, T., Morokuma, K., and Musaev, D. G. (2005) Elucidation of the mechanism of selenoprotein glutathione peroxidase (GPx)-catalyzed hydrogen peroxide reduction by two glutathione molecules: A density functional study, *Biochemistry 44*, 11864−11871.
40. Musaev, D. G., Geletii, Y. V., Hill, C. L., and Hirao, K. (2003) Can the ebselen derivatives catalyze the isomerization of peroxinitrite to nitrate?, *J. Am. Chem. Soc. 125*, 3877−3888.
41. Musaev, D. G., and Hirao, K. (2003) Differences and similarities in the reactivity of peroxinitrite anion and peroxynitrous acid with ebselen. A theoretical study, *J. Phys. Chem. A 107*, 1563−1573.
42. Prabhakar, R., Musaev, D. G., Khavrutskii, I. V., and Morokuma, K. (2004) Does the active site of mammalian glutathione peroxidase (GPx) contain water molecules? An ONIOM study, *J. Phys. Chem. B 108*, 12643−12645.
43. Frisch, M. J., et al. (2004) Gaussian 03 (Revision C1), Gaussian Inc., Pittsburgh, PA.
44. (a) Becke, A. D. (1988) Density-functional exchange-energy approximation with correct asymptotic behavior, *Phys. Rev. A 38*, 3098−3100; (b) Lee, C., Yang, W., and Parr, R. G. (1988) Development of the Colle-Salvetti correlation energy formula into functional of the electron density, *Phys. Rev. B 37*, 785−789; (c) Becke, A. D. J. (1993) Density-functional thermochemistry. III. The role of exact exchange, *Chem. Phys. 98*, 5648−5652.

45. Siegbahn, P. E. M., and Blomberg, M. R. A. (2000) Transition-metal systems in biochemistry studied by high-accuracy quantum chemical methods, *Chem. Rev. 100*, 421−437.
46. Cances, E., Mennucci, B., and Tomasi, J. (1997) A new integral equation formalism for the polarizable continuum model: theoretical background and applications to isotropic and anisotropic dielectrics, *J. Chem. Phys. 107*, 3032−3041.
47. Prabhakar, R., Blomberg, M. R. A., and Siegbahn, P. E. M. (2000) A density functional theory study of a concerted mechanism for proton exchange between amino acid side chains and water, *Theor. Chem. Acc. 104*, 461−470.

BI060456E